

Modelling the cardiac transverse-axial tubular system.

Michal Pásek, Jiří Jirumda, Georges Christé, Clive Orchard

► **To cite this version:**

Michal Pásek, Jiří Jirumda, Georges Christé, Clive Orchard. Modelling the cardiac transverse-axial tubular system.. Progress in Biophysics and Molecular Biology, Elsevier, 2007, 96 (1-3), pp.226-43. 10.1016/j.pbiomolbio.2007.07.021 . inserm-00326064

HAL Id: inserm-00326064

<https://www.hal.inserm.fr/inserm-00326064>

Submitted on 1 Oct 2008

HAL is a multi-disciplinary open access archive for the deposit and dissemination of scientific research documents, whether they are published or not. The documents may come from teaching and research institutions in France or abroad, or from public or private research centers.

L'archive ouverte pluridisciplinaire **HAL**, est destinée au dépôt et à la diffusion de documents scientifiques de niveau recherche, publiés ou non, émanant des établissements d'enseignement et de recherche français ou étrangers, des laboratoires publics ou privés.

For: Progress in Biophysics and Molecular Biology; focussed issue
Date of this version: 6th March 2007

Modelling the cardiac transverse-axial tubular system

M. Pásek^{*†}, J. Šimurda^{†§}, G. Christé[‡] and C.H. Orchard[¶]

* Institute of Thermomechanics, Czech Academy of Science - branch Brno.

† Department of Physiology, Faculty of Medicine, Masaryk University, Brno, Czech Republic

§ Department of Biomedical Engineering, Faculty of Electrical Engineering and Communication, Brno, Czech Republic

‡ INSERM Lyon, France

¶ Department of Physiology, University of Bristol, Bristol, BS8 1TD, United Kingdom

Correspondence to Clive Orchard at the above address[¶]
e-mail: clive.orchard@bristol.ac.uk
tel: +44-(0)117-331-7289

Running head: Modelling the TATS

Abstract

The transverse-axial tubular system (TATS) of cardiac ventricular myocytes is a complex network of tubules that arises as invaginations of the surface membrane; it appears to form a specialised region of cell membrane that is particularly important for excitation-contraction coupling. However much remains unknown about the structure and role of the TATS. In this brief review we use experimental data and computer modelling to address the following key questions: (i) What fraction of the cell membrane is within the TATS? (ii) Is the composition of the TATS membrane the same as the surface membrane? (iii) How good is electrical coupling between the surface and TATS membranes? (iv) What fraction of each current is within the TATS? (v) How important is the complex structure of the TATS network? (vi) What is the effect of current inhomogeneity on luminal ion concentrations? (vii) Does the TATS contribute to the functional changes observed in heart failure? Although there are many areas in which experimental evidence is lacking, computer models provide a method to assess and predict the possible function of the TATS; such models suggest that although the surface and TATS membranes are electrically well coupled, concentration of ion flux pathways within the TATS, coupled to restricted diffusion, may result in the ionic composition in the TATS lumen being different from that in the bulk extracellular space, and varying with activity and in pathological conditions.

Keywords: t-tubules; TATS; heart; calcium; ventricle; computer model

Introduction

The cardiac transverse-axial tubular system (TATS; also known as the t-tubules) is a complex network of membrane invaginations; it extends radially across ventricular myocytes from the surface of the cell to its centre, but also shows complex branching and longitudinal extensions (Soeller and Cannell, 1999). The functional importance of the TATS was first recognized in skeletal muscle, in which it extends radially over a longer distance and is narrower than in cardiac cells: extensive experimental work and modelling have shown conduction of excitation and changes of luminal ion concentrations in the TATS of skeletal muscle (e.g. Friedrich et al. 2001; see Caillé et al., 1985 for review).

For many years it was assumed that the TATS in cardiac ventricular myocytes was a simple continuation of the surface membrane that carried membrane depolarisation and excitation to the centre of the cell, allowing synchronous Ca release, and hence contraction. As a consequence, the TATS has not been incorporated into most computer models of cardiac myocytes (see Winslow et al., 2000; Puglisi et al., 2004 for review). However structural and functional studies suggest that the TATS is highly specialised for excitation-contraction coupling: many of the key proteins involved in trans-sarcolemmal Ca flux are located predominantly in the TATS, the Ca release sites of the cardiac sarcoplasmic reticulum are closely juxtaposed to the TATS, and Ca release occurs predominantly at the TATS (see Brette and Orchard, 2003; Song et al., 2005 for reviews).

The function of the TATS is further complicated because it represents a region of restricted diffusion, so that ion flux across the TATS membrane may alter ion concentrations within the TATS lumen. It has long been recognised that ion accumulation and depletion in inter-cellular clefts may be important in modulating cardiac electrophysiology (Attwell et al., 1979), and it has been suggested that such changes could occur within the TATS. However, evidence to support this idea has only been provided relatively recently (Bers 1983; Yasui et al., 1993; Tourneur et al., 1994; Clark et al., 2001). This is potentially important, since Ca handling proteins are located predominantly within the TATS, and are therefore exposed to luminal Ca; they may therefore be exposed to an extracellular Ca that differs from that in the bulk extracellular space, in the same way that they are exposed to an intracellular Ca, in the fuzzy space, that differs from that in the bulk cytoplasm.

Biophysically realistic computer models of the cardiac myocyte, incorporating a TATS (figure 1), can be used to explore these suggestions (Pasek et al., 2003; Pasek et al., 2006). However such models are only as accurate as the experimental data they are based on; experimental investigation of TATS

function has been hampered by its relative inaccessibility precluding, for example, patch clamp recordings from TATS membrane. However a method has recently been developed to physically and functionally detach the TATS from the surface membrane (detubulation) of cardiac ventricular myocytes. This allows the loss of current associated with the loss of TATS membrane to be quantified. At the same time, a 3D reconstruction of TATS has been provided for guinea-pig (Amsellem et al., 1994; Amsellem et al., 1995) and rat (Soeller and Cannell, 1999) myocytes.

These studies have provided data for species-specific computer models of rat (Pasek et al., 2006) and guinea-pig (Pasek et al., 2007b) ventricular cardiac myocytes incorporating TATS. These models have highlighted several important features of TATS function, and the potential importance of parameters that remain to be determined experimentally. The present review outlines the interaction between experimental and modelling work on the TATS, in particular, areas for further work, and possible approaches to these problems. Such interactive modelling will, we believe, suggest future experiments and reveal hidden variables and sources of artefacts, as it has in skeletal muscle, from Freygang et al., (1964) to Wallinga et al., (1999). The challenge with cardiac TATS is to model a labile, complex and tortuous 3D network of restricted diffusion, unknown membrane composition, and incompletely known protein composition and activity.

Figure 1 near here

1. What fraction of the cell membrane is within the TATS?

A fundamental question is the fraction of the cell membrane within the TATS. Early electron microscopy (EM) suggested ~30% (Page 1978), although preparation of tissue for EM may result in shrinkage and distortion of the tissue. This value received support, however, when it was shown that detubulation resulted in loss of ~32% of cell capacitance in rat ventricular myocytes, although when corrected for the presence of non-detubulated myocytes and incomplete detubulation, this value is slightly higher (Pasek et al., 2007a). However filling the TATS of a living rat ventricular myocyte with a fluorescent indicator, and imaging using 2-photon confocal microscopy, showed that TATS membrane comprises $0.44 \mu\text{m}^2$ per μm^3 cell volume (Soeller and Cannell, 1999). This can be normalised to total surface area per μm^3 , calculated either from the cell dimensions ($0.68 \mu\text{m}^2/\mu\text{m}^3$; (Soeller and Cannell, 1999) or from electrophysiological measurements of cell capacitance ($0.68 - 0.89 \mu\text{m}^2/\mu\text{m}^3$; (Satoh et al., 1996)) assuming a membrane specific capacitance of $1 \mu\text{F}/\text{cm}^2$; this gives the

percentage of cell membrane within the TATS as 65 – 49%: higher than estimates obtained by other means.

However all of these approaches pose problems. The problems with tissue preparation for EM are well recognised, and the problems of incomplete detubulation are outlined above. Less well recognised is the problem of measuring cell membrane area. If calculated using optical methods, both cell surface and TATS membrane area may be underestimated unless membrane convolution is taken into account. This may occur, for example, at the intercalated disks due to membrane folding, and in the TATS due to the presence of caveolae. The former will increase the apparent percentage of membrane in the TATS (by underestimating the surface membrane area); the latter will tend to underestimate the percentage of membrane in the TATS. An alternative method is to measure membrane capacitance before and after detubulation, and calculate membrane areas assuming a specific capacitance of $1 \mu\text{F}/\text{cm}^2$. However this assumes that specific capacitance is uniform across the cell membrane; if, for example, the specific capacitance of the TATS membrane is lower than that of the surface membrane, total membrane area as well as the percentage of membrane in the TATS will be underestimated. A further complication is that measurements of cell capacitance are prone to artefacts (see companion paper; Pasek et al., 2007a).

In addition to methodological problems, there may be differences due the species, age and health of the animals used, all of which appear to alter the TATS, which is remarkably labile. Despite methodological problems and considerable variability, modelling the TATS may help to determine possible sources of discrepancies and to decide which of the estimates may be closest to correct.

The companion paper to this review (Pasek et al., 2007a) shows one approach to this problem, using a model of the rat ventricular myocyte (Pasek et al., 2006) to find parameters for the TATS that reconcile optical data (Soeller and Cannell, 1999) and functional data from detubulation. This shows that a model with a fractional area of TATS of 49% can comply with data from both experimental approaches if incomplete detubulation (~8% of TATS remaining after detubulation) and lower specific capacitance of tubular membrane ($0.56 \mu\text{F}/\text{cm}^2$) are incorporated, although there are uncertainties even with this estimate.

2. Is the composition of the TATS membrane the same as the surface membrane?

The considerations in the previous section suggest that if the specific capacitance of the TATS membrane is lower than that of the surface membrane it might help to reconcile differences between electrical and optical measurements of the fraction of membrane in the TATS. If the specific capacitance of the two membranes is different, it is likely to be because of differences in the composition of the two membranes. This would be important because it will determine the electrical properties of the membrane itself, and because membrane composition alters the function of membrane proteins.

The TATS appears to be formed by lipid rafts, and the t-tubules are rich in caveolae (above), which have a high cholesterol content, suggesting that the TATS membrane may be rich in cholesterol. It has previously been shown that skeletal t-tubule membrane has a high cholesterol content (Roseblatt et al., 1981; Sumnicht and Sabbadini, 1982), but the composition of the cardiac TATS membrane is unknown. A recent study using the cholesterol-depleting agent methyl- β -cyclodextrin showed no acute change in t-tubule structure in rat ventricular myocytes (Calaghan and White, 2006), although previous work has shown that the same agent disrupts the t-tubules in myotubes (Pouvreau et al., 2004); it is possible that the structure of cardiac and skeletal t-tubules rely to different extents of cholesterol or that changes in structure require longer or are more subtle than the observations in rat myocytes allowed. It might be expected that insertion of cholesterol in the membrane would increase membrane thickness, and thus decrease capacitance. However previous work investigating the effect of cholesterol on membrane capacitance has shown either a decrease, no change, or increase in membrane capacitance, although some of these studies used artificial lipid membranes which, although a useful experimental system, differ from the cell membrane in many ways. Although a recent study showed that methyl- β -cyclodextrin has no effect on cell capacitance in rat ventricular myocytes (Calaghan and White, 2006), it remains unclear whether the composition of the TATS membrane differs from that of the surface membrane and if so, in what way, and if its cholesterol content is higher, the effect this has on membrane capacitance.

3. How good is the electrical coupling between the surface and TATS membranes?

This is an important question because much of our knowledge of cellular cardiac electrophysiology has been obtained using the voltage clamp technique in mammalian ventricular myocytes. Poor electrical coupling between the TATS and surface membranes, or propagated responses along the TATS membrane, could result in voltage escape within the TATS. Such loss of voltage control would result

in erroneous current-voltage relations whereas tight electrical coupling between the membranes would ensure synchronous changes of membrane potential across the whole cell membrane.

Cable theory provides a useful framework to consider voltage control in the subthreshold range: membrane voltage remains uniformly distributed along a fibre provided the fibre length, l , is much shorter than the space constant λ ($l/\lambda \ll 1$). This condition is met for the whole cardiac cell: using approximate dimensions of $100 \times 20 \times 6 \mu\text{m}$, a specific resistivity of the intracellular medium of $200 \Omega/\text{cm}$ and a specific membrane resistance $6.7 \text{ k}\Omega/\text{cm}^2$ (Daut 1982), then $\lambda = 0.88 \text{ mm}$ so that $l/\lambda = 0.11$. Since the TATS lumen is open to the extracellular medium, and the inner face of the TATS membrane faces the cytoplasm, it seems reasonable to use a specific resistance of $83 \text{ M}\Omega/\text{cm}$ (measured in Tyrode solution) to calculate the passive electrical parameters of the t-tubule membrane. Representing the t-tubules as cylinders with a radius of 127 nm , a maximal length of $25 \mu\text{m}$, and assuming the same specific membrane resistance as the surface membrane ($6.7 \text{ k}\Omega/\text{cm}^2$), then $r_{mt} = 84 \Omega/\text{cm}$ and $r_t = 164 \text{ G}\Omega/\text{cm}$ (membrane resistance and intra-tubular resistance per unit t-tubule length, respectively). It follows that the tubular space constant can be estimated as $\lambda_t \equiv \sqrt{r_{mt}/r_t} = 226 \mu\text{m}$ and thus $l_t/\lambda_t = 0.11$. Thus it appears likely that membrane voltage is spatially uniform within the TATS.

These results are consistent with experimental data showing a single exponential decay of the whole cell capacitance current obtained in response to small, subthreshold, voltage clamp steps (Sato et al., 1996): a propagated response in the TATS would be expected to result in significant deviation from a monoexponential time course. Further support for synchronous polarization of the TATS membrane is provided by a model of the voltage clamped cardiac cell with a compartment representing the TATS (Pasek et al., 2007b). This shows that the current response to a subthreshold voltage step consists of two exponentials: a very small component with a time constant of $\sim 1 \mu\text{s}$, due to the connection between the surface and TATS membranes; its magnitude was $\sim 2\%$ of the main component with a time constant approaching the product of the series resistance and the capacitance of the total membrane system. Thus, the response was practically monoexponential.

Use of the space constant as a criterion for spatial voltage uniformity within the TATS may be questioned, because the membrane resistance r_m is variable and declines markedly in the suprathreshold voltage range. It is therefore better to estimate the maximum voltage difference between the ends of the t-tubule (ΔV_{max}) assuming AP propagation with a constant velocity (θ). Membrane voltage as a

function of space (x) and time (t) can be expressed as $V(x,t) = V(x - \theta \cdot t)$ and consequently its partial derivatives with respect to both variables will exhibit the relation $-\partial V/\partial x = \theta^{-1} \partial V/\partial t$. This relation holds true for maximal values in the form $|dV/dx|_{\max} = \theta^{-1} (dV/dt)_{\max}$ where $(dV/dt)_{\max}$ means maximum velocity of AP depolarization. It follows that $|dV/dx|_{\max} l$ and thus $\theta^{-1} (dV/dt)_{\max} l$ is the upper limit of the membrane voltage difference along a t-tubule of length l which is expressed by the relation $\Delta V_{\max} \leq \theta^{-1} (dV/dt)_{\max} l$. If $(dV/dt)_{\max} = 160$ V/s and $\theta = 1$ m/s, the voltage drop along the tubule does not exceed 4 mV for maximum tubule length $l_{\max} = 25$ μm and 1.12 mV for mean tubule length $l = 7$ μm .

Thus the membrane potential is likely to be uniform during all but the largest and fastest changes of membrane voltage induced either experimentally, by voltage clamp, or during physiological activation of membrane currents. In support of this idea, it has recently been shown that time to peak I_{Na} is unaltered at different potentials following detubulation and is independent of series resistance in control and detubulated myocytes (Brette and Orchard, 2006a). This lack of change in the characteristics of I_{Na} following detubulation, and their independence of series resistance, are consistent with good voltage control of the t-tubule membrane.

Figure 2 near here

However, the uniformity of membrane voltage as a consequence of tight electrical coupling of the surface and TATS membranes does not imply that identical action potentials would be generated separately by the surface membrane and TATS. Computer modelling suggests that the AP generated by the TATS membrane is considerably longer than that generated by the surface membrane when the electrical coupling of the 2 membranes is disrupted (Figure 2). This disruption was simulated by forcing the current circulating through both membranes (I_{circ} in Pasek et al., 2006) to zero; this current tends to minimize differences in the APs of coupled membranes. The difference in AP duration in the two membranes is a consequence of the different concentrations of ion flux pathways: L-type Ca channels, which are preferentially located in the TATS membrane, are mainly responsible for the increased AP duration. In the rat ventricular myocyte model (Fig. 2B) the contribution of other unequally distributed channels or carriers appeared to be insignificant. However, due to tight electrical coupling the duration of the whole cell AP lies between the trajectories generated by the isolated

membranes (figure 2B). This agrees well with recent experimental results comparing action potentials recorded before and after detubulation (Figure 2A; Brette et al., 2006c).

4. What fraction of each current is within the TATS?

Modelling the TATS is critically dependent on the fraction of each current located within the TATS membrane. Immunohistochemistry has been widely used to show the localisation of membrane proteins within cardiac myocytes. Although useful, immunohistochemistry is not without its problems (Brette and Orchard, 2003), but critically is unable to report protein function, which depends not only on the presence of the protein, but also on local environment, the presence of accessory proteins and local protein regulation; it is also difficult to quantify. Although immunogold labelling can overcome some of these problems, there are relatively few studies using this technique to investigate protein localisation within the TATS, and even this technique cannot report function.

A different approach is detubulation. This allows quantification of the current lost when the TATS are detached from the surface membrane. Such quantification requires correction for incomplete detubulation, which assumes that the remaining TATS membrane has the same protein composition as that which has been lost; i.e. that proteins are homogeneously distributed throughout the TATS membrane. This is, however, unlikely: using immunohistochemistry it has been shown that TATS appear to have (at least) 3 domains; one containing L-type Ca channels, adjacent to ryanodine receptors in the sarcoplasmic reticulum membrane, one containing the Na/Ca exchanger, and one containing Na channels (Scriven et al., 2002). The Na/Ca exchanger may also be differentially localised between the transverse and longitudinal elements of the TATS (Thomas et al., 2003).

Despite these problems, both immunohistochemistry and detubulation, as well as other techniques (see Brette and Orchard, 2003 for review), have shown that many membrane proteins and currents are not evenly distributed between the surface and TATS membranes. For example, I_{Ca} , Na/Ca exchange and the Na/K ATPase have all been shown predominantly in the TATS membrane, whereas most, but not all, K currents appear to be more evenly distributed (see Brette and Orchard, 2003 for review). It also appears that there is heterogeneity of distribution within the TATS (above).

The extent to which protein function (membrane currents) reflects protein distribution between the TATS and surface membranes is unclear and may vary depending on conditions. Local modulation of protein function may result in protein function showing a different distribution from the proteins

themselves. There are several factors that might bring about such local modulation: (i) local ion gradients. It is generally accepted that there is probably a space with restricted diffusion at the inner face of the cell membrane close to ion flux pathways (fuzzy space), in which the ion concentration may be markedly different from that in the bulk cytoplasm. Similarly, the TATS lumen represents a restricted diffusion space with a high concentration of ion flux pathways in the adjacent TATS membrane. Thus ion concentration changes may occur in the TATS lumen, which may alter the function of the adjacent proteins. Thus both the extracellular and intracellular ion concentrations to which a membrane protein is exposed are unknown. (ii) protein regulation. Many proteins that mediate trans-membrane ion flux are regulated, either by accessory proteins or by phosphorylation. It is not clear, however, that either of these are the same at the TATS and surface membranes. It has not been demonstrated that the same accessory proteins are present to the same extent in the two membranes. It has however been shown that protein regulation at the two sites may be different. For example, many of the key proteins involved in the beta-adrenergic pathway appear to be located predominantly at the TATS (Laflamme and Becker, 1999), and it has been demonstrated that activation of the beta-2 adrenergic pathway produces local phosphorylation and stimulation of I_{Ca} (Davare et al., 2001). Comparison of the response of I_{Ca} to beta-adrenergic stimulation in control and detubulated myocytes suggests that I_{Ca} is better coupled to the beta-adrenergic pathway in the TATS than at the surface membrane (Brette et al., 2004a). In the presence of tonic activity of this pathway, this would result in increased activity in the TATS compared to the surface membrane. (iii) isoform distribution. Many cardiac ion channels exist with several isoforms within a single cell. It has recently been shown that the TTX-sensitive and TTX-resistant isoforms of the voltage gated Na channel have markedly different distributions between the TATS and surface membranes (Brette and Orchard, 2006b). These channels also have different electrophysiological characteristics, making it likely that I_{Na} is different in the two membranes. It is unknown whether such differences exist for other channels types. (iv) dyadic function. Ca influx via L-type Ca channels triggers Ca release from adjacent sarcoplasmic reticulum. The released Ca contributes to inactivation of the Ca channels. Although the amount of Ca released for a given trigger appears to be the same at the TATS and surface membrane, this feedback inactivation appears to be more potent at the TATS (Brette et al., 2004b). The reason for this is unknown: it may be due to differences in the channel isoform, or in channel regulation due, for example, to the presence or absence of factors such as calmodulin, or it may be due to differences in dyadic structure at the two sites. Whatever the explanation, this represents a further difference between the function of proteins at the TATS and surface membranes, which needs to be accounted for in models of the TATS.

Figure 3 near here

Thus the distribution of protein function between the TATS and surface membranes depends on a multitude of factors in addition to protein distribution. For many proteins the distribution of function is unknown: for example there have been relatively few studies of the distribution of K currents, and those studies that exist are in species that have different K channel expression and action potential morphology from the human. For membrane currents whose distribution is known, the extent to which it is due to factors other than protein distribution is unclear. Even if the distributions are known, their density will remain unknown until good estimates of TATS membrane area, and knowledge of the heterogeneity of protein distribution within the TATS is elucidated. However computer models of the TATS can be used to explore the potential importance of the distribution of function of particular proteins as well as the importance of other parameters of TATS membrane. This is demonstrated in Figure 3, which compares simulations during 5 Hz steady-state stimulation in a rat model (Pasek et al., 2006) with simulations obtained after modifying the model to reconcile data obtained using optical techniques and detubulation (see Pasek et al., 2007a; section 1, above, and the legend to table 1, for further explanation). The original experimental data, and the model settings, including the fractional area of membrane within the TATS, the specific capacitance of the TATS membrane and the distribution of ion currents in the TATS membrane, are shown in table 1. Reducing the fractional area of the TATS from 56% to 49% had only a small effect on function (not shown); however reducing the specific capacitance of the TATS membrane from 1 to 0.56 $\mu\text{F}/\text{cm}^2$, as well as altering the distribution of currents between the TATS and surface membranes to agree with recent data obtained by detubulation, altered action potential configuration and the Ca transient. These complex effects are due partly to a reduction of capacitance current due to the lower specific capacitance of the TATS, and to greater modulation of tubular ionic currents by the larger changes of tubular ion concentrations induced by the greater fractions of currents in the TATS. This reconstruction of experimental data suggests two important points: First, the fractions of ion flux pathways in the TATS could be even higher than suggested by loss of membrane currents following detubulation, because of incomplete detubulation, changes in the concentration gradient across the tubular membrane, and contamination by incompletely blocked currents. Secondly, the distribution of ion currents between the TATS and surface membranes plays an important role in modulation of the electrical activity of the cardiac cell and its inotropic state.

5. How important is the complex structure of the TATS network?

Soeller and Cannell (1999) showed that in a living rat ventricular myocyte the TATS consists of a complex branching network of tubules, with diameters from 20 to 450 nm, and with a mean inter-branch segment length of 6.87 μm . This organization of the TATS enables rapid propagation of electrical excitation into the cell interior. However, the complexity of the TATS appears to slow ion exchange between the TATS lumen and extracellular space (Yao et al., 1997; Shepherd and McDonough, 1998; Blatter and Niggli, 1998; Swift et al., 2006) and to cause significant depletion or accumulation of ions within the TATS lumen.

Functionally, the restricted diffusion space of the TATS has been investigated by monitoring the rate of change of Na and Ca currents following a rapid change of [Na] or [Ca] respectively at the cell surface (Shepherd and McDonough, 1998). These experiments showed that I_{Na} and I_{Ca} changed with a time course that could be defined by a fast time constant (~ 25 ms), ascribed to changes in the current at the cell surface, and a slower time constant (~ 200 ms), interpreted as the rate of Na and Ca diffusion into the TATS. However (Blatter and Niggli, 1998), using a membrane-bound Ca indicator, reported that wash-out of Ca from the TATS of guinea-pig ventricular myocytes occurred with a $t_{1/2}$ of 0.9 s at the surface and 1.7 s in the deeper regions of the TATS which, assuming a single exponential time course, gives time constants of 1.3 s and 2.46 s: slower than the value derived from measurements of I_{Ca} (Yao et al., 1997; Shepherd and McDonough, 1998). The reasons for the discrepancy are not clear, although the membrane bound Ca indicator may itself slow the time course of diffusion. For K, it appears that a single exponential time course can account for the diffusion of K within the TATS that underlies changes in resting potential or whole cell current in response to a relatively small step change in bathing [K] (Yao et al., 1997; Swift et al., 2006; Pasek et al., 2006). Total K removal results in transient hyperpolarization of the resting membrane potential, probably due to the negative shift in the K reversal potential, followed by depolarization as I_{K1} decreases (G. Christé and C. Chouabe, unpublished). The whole cell current during transient perfusion with 0 mM K while voltage ramps were applied shows a fast decay but slow restoration of inward current at -140 mV upon restoration of K (> 10 s for 95% completion; G. Christé and C. Chouabe, unpublished). This suggests that diffusional exchange of K ions in the TATS may be slower than previously suggested.

The factors that determine the rate of ion diffusion within the TATS, and hence the rate of ion exchange between the TATS lumen and the bulk extracellular space, include the varying diameter and tortuous structure of tubules throughout the cell, ion buffering by the TATS membrane, and ion transport by ion flux pathways. To demonstrate the effect of changes of tubular diameter on the rate of

ion exchange and the velocity of propagation of a concentration gradient along a tubule we designed a simple model of a 10 μm long tubule divided into five concentric compartments with variable diameters. Using this model we could obtain an approximate solution of the diffusion equation:

$$\frac{\partial[\text{Ca}^{2+}]_t}{\partial t} = D_{\text{Ca}} \frac{\partial^2[\text{Ca}^{2+}]_t}{\partial x^2}.$$

The traces in Figure 4 show the increase of [Ca] in the peripheral, central and deep sections of the tubule when the external [Ca] is rapidly increased from 0 to 1 mM. The basic simulation (black lines) was performed using the model with uniform diameter (300 nm) along the tubule and a diffusion coefficient, D_{Ca} , of $0.95 \cdot 10^{-6} \text{ cm}^2/\text{s}$ characterising the apparent rate of ion diffusion in TATS (Shepherd and McDonough, 1998). Using this “slow” diffusion coefficient, the time needed for a 50 % change of ion concentration in the peripheral section was 45 ms, but was 340 and 480 ms in the central and deep sections, respectively. The mean velocity of propagation of ion concentration gradient along the tubule was 18.4 $\mu\text{m}/\text{s}$, which is close to the range reported by Blatter and Niggli (1998; 3.4-16.3 $\mu\text{m}/\text{s}$) for guinea pig TATS. The next series of simulations (red lines) used $D_{\text{Ca}} = 7.9 \cdot 10^{-6} \text{ cm}^2/\text{s}$ characterising “fast” Ca diffusion as measured in bulk extracellular space (Marcus 1997). Using this coefficient with uniform diameter led to a rapid change of tubular ion concentrations in all compartments (first panel). However, reducing peripheral tubule diameter from 300 to 100 nm (second panel) or increasing the diameter of one of the subsequent sections of the tubule from 300 to 450 nm (third panel) led to substantial slowing of ion concentration changes along the tubule. Thus reduction of tubular diameter decreased total flux of ions diffusing in the deeper parts of the tubule, while increasing diameter slowed down the ion concentration changes in the dilated and adjacent compartments.

Figure 4 near here

The interplay of these effects is shown in the fourth panel of figure 4, which demonstrates that variations of tubular diameter alone are sufficient to induce very similar effects to those observed when a “slow” apparent diffusion coefficient ($D_{\text{Ca}} = 0.95 \cdot 10^{-6} \text{ cm}^2/\text{s}$) is used. The effect of increasing the diameter of a deeper part of the tubule can also be produced by ion buffering in TATS. However, until the potency of ion buffers in the TATS is determined experimentally the effect of these mechanisms is unclear and difficult to analyse.

6. The effect of current inhomogeneity on luminal ion concentrations

The data presented in the previous sections suggest that many trans-membrane ion flux pathways are located predominantly within the TATS, where they are inhomogeneously distributed, and that the TATS represent a restricted and complex diffusion space. This may have important consequences for the concentration of ions within the TATS lumen. For example, of the ion flux pathways investigated to date, I_{Ca} is perhaps the most concentrated within the TATS, where it is found adjacent to ryanodine receptors and serves to initiate contraction of the cardiac cell. Of the sarcolemmal ion flux pathways, channels have the highest rate of ion flux. It might be predicted, therefore, that during increased activity, activation of I_{Ca} , coupled to restricted diffusion from the extracellular space, might decrease luminal $[Ca]$, and thus I_{Ca} , particularly since Ca efflux pathways do not appear to be as concentrated in the TATS membrane and are therefore likely to be less effective in returning Ca to the lumen. This would have two important consequences: first, it would act as negative feedback to reduce Ca influx. This would limit contraction by decreasing the trigger for Ca release and Ca loading of the cell by I_{Ca} ; this may therefore play a role in cellular Ca homeostasis and help reduce Ca overload at high heart rates. Secondly, if Ca within the lumen decreases sufficiently it may remain below bulk extracellular concentration; this would result in continuous Ca flux from the extracellular space into the TATS lumen. In order for this situation to be maintained at steady-state, this Ca must be continuously removed from the lumen, which can only occur across the cell membrane. This implies that Ca may cycle from the TATS membrane to the surface membrane during activity.

These consequences of Ca channel localisation within the TATS and restricted diffusion have been observed in a model of the rat ventricular myocyte including TATS as a single compartment (Pasek et al., 2006). If the model cell was stimulated at 5 Hz, mean tubular Ca concentration at steady state was ~6 % lower than the bulk extracellular concentration. This decreased Ca transient amplitude by ~25%, when compared with maintaining ion concentrations constant in the TATS at the extracellular level. Ca (and Na and K) cycling from the TATS membrane to the surface membrane during activity was also observed and analyzed using a model of the guinea pig myocyte (Christé et al., 2005). At 4 Hz steady-state stimulation the amount of Ca cycling was estimated to be 17 % of the Ca transferred across the cell membrane by I_{Ca} .

A question arises whether non-homogeneous ion channel distribution would exacerbate these predicted effects. Clustering of ion channels may cause higher local transmembrane ion flux and hence greater local ion depletion within the TATS lumen than for homogeneous distribution of the same number of

channels. However it has not, to date, been possible to test this prediction experimentally. Computer models of the TATS allow these predictions to be explored if the t-tubules are regarded as a system with parameters distributed in space. The present models representing TATS as a single compartment lack this ability. However, simulations based on solution of partial differential equations suggest that clustering of calcium channels at dyads has little effect on the distribution of Ca along the t-tubules (Simurda et al., 2004). In these simulations, we explored the effect of clustering of Ca channels at dyads and of Ca-buffering: the glycocalyx and proteins present at the luminal surface of the TATS membrane (Kostin et al., 1998) are able to bind Ca reversibly, thus acting as Ca buffers and altering Ca dynamics in the TATS lumen. When we investigated two clusters of Ca channels separated at two dyads along a t-tubule represented by a cylinder, non-homogeneous Ca-depletion was prominent during the first 60 ms; however due to the effects of diffusion and Ca-buffering, this became negligible 150 ms after activation of I_{Ca} . In later simulations (Simurda, unpublished), clusters of Ca-channels were distributed according to the reported minimum distance between dyads of 414 nm (Franzini-Armstrong et al., 1999). In this case the irregularities of Ca depletion practically disappeared even in the absence of Ca buffers; for comparison the simulation was repeated assuming uniformly distributed I_{Ca} transferring the same electrical charge across the t-tubular membrane. The distribution of Ca depletion with distance along the t-tubule was practically the same as in the case of clustering channels within dyads. Greater local depletion in the regions adjacent to dyads was compensated by less depletion in the neighbouring segments and the Ca gradients were rapidly equalized by diffusion. However, the real situation is further complicated by the absence of Ca-channels in axial components of the TATS. In contrast, Na/Ca exchangers have been reported to be distributed in clusters predominantly out of dyads and caveolae in transverse and axial components of the TATS (Scriven et al., 2002; Thomas et al., 2003). In addition, co-localization of recently discovered Ca-permeable non-specific cation channels (CRPC3) with Na-Ca exchanger, Na channels and Na-K pump has been shown in the axial component of the TATS in rat cardiomyocytes (Goel et al., 2006). The proximity of these proteins, which will affect Ca concentration in the lumen of the axial component of the TATS, to SERCA in the longitudinal components of sarcoplasmic reticulum, may also affect Ca homeostasis. Detailed modelling of spatial and temporal distribution of ionic concentrations in the TATS lumen is needed, considering geometric irregularities (variable radius, caveolae) and inhomogeneities in distribution of all ion transporting proteins.

7. Does the TATS contribute to the functional changes observed in heart failure?

There have been several recent reports that the structure of the TATS can change during heart failure in animal models and humans. Animal models of heart failure (canine tachycardia-induced dilated cardiomyopathy: He et al., 2001, Balijepalli et al., 2003; rabbit: Quinn et al., 2003; SHR rats: Fowler et al., 2006, Song et al., 2006) show gaps in the TATS network. In ventricular myocytes from failing human hearts, disorganization of the TATS has been reported (Cannell et al., 2006) with a decrease in the fraction of tubules properly aligned at the Z-lines, which has also been reported in failing myocytes from a canine model of heart failure (He et al., 2001; Balijepalli et al., 2003) and in SHR rats (Song et al., 2006). These data not only show that TATS' structure is labile but also suggest that changes in the TATS may contribute to the changes of function observed during failure, and it is notable that myocytes from failing hearts show many functional similarities to detubulated cells.

Work to date suggests that changes in the structure of the TATS have two main effects. First "gaps" in the TATS network result in areas in which Ca is not released rapidly by Ca influx; instead a wave of Ca-induced Ca release invades these areas from adjacent regions (Louch et al., 2004; Song et al., 2006). This decreases the synchronisation of Ca release, and thus decreases and slows the Ca transient (Louch et al., 2004); it also suggests "orphan" ryanodine receptors in these areas, which can release Ca but are not located adjacent to Ca channels (Song et al., 2006). Secondly, it has been suggested that these changes in the TATS are accompanied by changes in the structure of the dyad, so that Ca influx is less effective in triggering Ca release from adjacent sarcoplasmic reticulum, possibly because of an increase in the distance between the Ca channel and ryanodine receptors (Gomez et al., 2001; Cannell et al., 2006). Experimental data therefore suggest that changes in both the gross structure and the ultra-structure of the cardiac TATS may play a role in the functional changes in heart failure. There are however other ways in which changes in the structure of the TATS may alter cell function: (i) by altering the rate of diffusion exchange with the bulk extracellular space. It appears likely that concentration of ion flux pathways in the TATS and restricted diffusion with the bulk extracellular medium will result in changes of ion concentrations in the TATS lumen (above). This may be protective in the normal heart: Ca depletion in the TATS may help limit Ca overload, and K accumulation will tend to increase the conductance of K channels and activate the Na/K pump. Both effects would shorten action potential duration, and thus help protect the cell from the adverse effects of Ca overload and action potential prolongation, which may contribute to defective excitation-contraction coupling and arrhythmias. Indeed, the presence of TATS in a ventricular myocyte model may moderate the arrhythmogenic effects of hypokalaemia (Pasek et al., 2002), and in a model of the guinea-pig ventricular myocyte, suddenly fixing TATS concentrations to bulk extracellular values

caused a progressive increase in sarcoplasmic reticulum Ca load (Pasek et al., 2007b). These mechanisms may be impaired in myocytes from failing hearts because of loss of part of the TATS and/or a decrease in the density of Ca or K channels. Alternatively, they may be enhanced if diffusion times are increased, for example by increased disorganisation, tortuosity and narrowed lumens, and/or channel expression or activity are increased. However in the absence of experimental data it is difficult to predict the role of the TATS in cells from the failing heart.

Figure 5 near here

(ii) by changes in protein expression, distribution and regulation within the TATS. It is well documented that there are changes in ion flux pathways during heart failure e.g. (He et al., 2001; Quinn et al., 2003) For example the total number of Ca channels decreases whereas the whole cell Ca current density remains the same (He et al., 2001), probably due to increased Ca channel availability and open probability (Schroder et al., 1998). It appears possible, therefore, that the expression, distribution and regulation of membrane proteins changes. Although changes in the expression and regulation of membrane proteins have been reported during failure, there have been no studies investigating changes in the distribution of protein function between the TATS and the surface membrane in heart failure. Such changes in distribution could be brought about by changes in the expression or trafficking of ion transport proteins, by localised phenotype switching, changes in the expression or distribution of accessory proteins or protein regulation. Although all of these changes have been reported to occur in the whole cell, it is not known whether they might be localised and thus alter the distribution of protein function, with the functional consequences of protein localisation in the TATS (above). (iii) if $I_{K,ATP}$, which is activated during metabolic inhibition (Nichols and Lederer, 1991; Weiss and Venkatesh, 1993; Knopp et al., 1999), is located within the TATS. This is a large conductance channel which, when open, “clamps” the membrane potential, causing failure of the action potential and hence contraction (Cole et al., 1991) and in doing so helps preserve ATP within the cell. Figure 5 shows that in adult rat ventricular myocytes, the $I_{K,ATP}$ channel isoform Kir6.2 (and the inward rectifier I_{K1} channel isoform Kir2.1) co-localise with alpha-actinin along the t-tubules. These data are consistent with the observation that I_{K1} and $I_{K,ATP}$ decrease in parallel to the capacitance decay due to progressive detubulation of ventricular cardiac myocytes in primary culture (Christé 1999). In addition, significant labelling for Kir2.1 can be observed parallel to the long axis of the cell (panel A2), which is almost absent for Kir6.2 (A1). Although it is not yet clear whether the different distribution of Kir2.1 and Kir6.2 between the transverse and longitudinal elements of the TATS has functional implications, these

data do suggest that $I_{K,ATP}$ may be located predominantly within the TATS. This is consistent with data obtained using a scanning patch clamp technique, in which this current was found to be associated with TATS openings on the cell surface (Korchev et al., 2000). Given the large conductance of this channel and its concentration at the TATS membrane, it seems likely that metabolic inhibition, and the subsequent opening of this channel, may result in marked K efflux and accumulation within the TATS lumen. This would lead to development of inward tail current following rapid repolarisation, as shown to occur when $I_{K,ATP}$ is activated by metabolic blockade (Yasui et al., 1993), pharmacological stimulation (Tourneur et al., 1994) or anoxia (Knopp et al., 1999).

Modelling this phenomenon using our guinea pig model showed that $I_{K,ATP}$, elicited by a decrease of intracellular ATP concentration from 6.8 to 0.1 mM, induces a marked increase of tubular K concentration, which reached ~ 25 mM during a 50 ms voltage clamp from -85.5 mV to 40 mV (not shown). Its subsequent decrease to baseline at the end of the pulse induced a large inward I_{K1} tail current. In current clamp experiments, activation of $I_{K,ATP}$ during metabolic inhibition induces prominent action potential shortening (and reduction of twich amplitude) in guinea pig ventricular myocytes (Nichols and Lederer, 1991), which can be reproduced by incorporating $I_{K,ATP}$ into the Luo-Rudy model of the ventricular action potential (Ferrero et al., 1996).

Figure 6 near here

To explore whether accumulation or depletion of tubular ions is involved in action potential shortening following activation of $I_{K,ATP}$, we repeated these simulations using our guinea pig model including TATS (see a full description of the model in Pasek et al., 2007b). Action potentials were simulated in the model when ion concentration changes in TATS were allowed and when they were fixed at extracellular levels ($[Ca]_e = 1.8$ mM, $[K]_e = 5.4$ mM, $[Na]_e = 140$ mM) at normal $[ATP]$ concentration (6.8 mM) and when it was decreased to 1 and 0.5 mM (figure 6). In agreement with previous modelling (Ferrero et al., 1996; Shaw and Rudy, 1997), activation of $I_{K,ATP}$ resulted in a substantial reduction of action potential duration (APD). However, the reduction was greater when ion concentrations were allowed to change within the TATS. Perhaps surprisingly, this effect was predominantly caused by greater depletion of tubular Ca (by 24.4% and 31.3% at $[ATP]_i = 1$ and 0.5 mM respectively, versus 16.2% in control) induced by increased I_{Ca} with a reduction of the voltage during the action potential plateau (consistent with the I-V characteristics of guinea pig I_{Ca} shown by Grantham and Cannell, 1996). Increased accumulation of tubular K (by 13.5% and 20.3% at $[ATP]_i = 1$ and 0.5 mM

respectively, versus 7% in control), resulted in a slow phase of repolarisation of membrane potential to resting level at the end of the action potential. Although the effect of $I_{K,ATP}$ -induced accumulation of tubular K on action potential configuration is small during current clamp in the isolated cardiac cell, its role may be greater *in situ* where the compromised tissue may be in conditions close to voltage clamp, due to surrounding healthy tissue, in which greater K accumulation is observed (above) and where it could contribute to dispersion of electrical activity in the tissue, and hence the genesis of re-entrant arrhythmias

In addition to the consequences of failure discussed above, it is well known that many other aspects of cell function are affected in failure, including membrane transport, cellular ionic homeostasis, and altered electrical activity (e.g. Gao et al., 2005; Dos Remedios et al., 2003; Marks 2003; Wehrens and Marks, 2004; Sipido and Eisner, 2005). To simulate the complexity of these events requires integration of these changes into existing models, in addition to changes in the distribution of membrane ion transporters and TATS structure.

Conclusions and challenges for future experiments

Although the importance of the TATS is clear, it is also clear that there is much that remains unknown. Computer models can help us explore the role and importance of different factors in TATS function, and examples of such exploration are given above. Such exploration helps us to target and refine experiments.

There are technical challenges that will need to be addressed, and questions to be answered, for the role of the TATS to be fully elucidated. Current challenges are to measure the concentration of ions in the TATS lumen; to determine the composition of the t-tubule membrane, especially its lipid and protein composition; to make patch clamp recordings from TATS membrane; to define the changes that occur during development and in pathological conditions. Our current knowledge also begs further questions about how the TATS forms, why it is so labile, how proteins are trafficked and anchored there, how their attachment and location influences their function, and how proteins co-localise: the stoichiometry of the L-type Ca channel and ryanodine receptor appears to be the same at the TATS and surface membranes (Brette et al., 2006c); the mechanism is unknown. Future modelling of TATS function should take into account the complex geometry and inhomogeneities in the composition of the TATS including heterogeneities in the distribution and regulation of membrane proteins and lipid rafts

(Simons and Eehalt, 2002 for review) and will probably require an approach similar to that described recently for quantitative analysis of transport in the microcirculatory system as described by a structural database (Beard 2001). The cell interior would be represented by a discrete cubic lattice of inhomogenous elements. Such a complex model respecting real cell microstructure could then contribute to the Physiome Project of the International Union of Physiological Sciences (Bassingthwaighte 2000; Hunter et al., 2002; Bassingthwaighte and Vinnakota, 2004; Crampin et al., 2004; Beard et al., 2005; Hunter and Nielsen, 2005). As always, new challenges appear from answered questions; the combination of experimental and computational approaches promises to be particularly powerful in understanding the function of the TATS.

Acknowledgements

CHO is grateful to the British Heart Foundation and the Wellcome Trust for their financial support of work on the TATS. MP's work is supported by project AV0Z 20760514 from the Institute of Thermomechanics of Czech Academy of Sciences and project MSM 0021622402 from the Ministry of Education, Youth and Sports of the Czech Republic; MP is also grateful to the Physiological Society for their award of a Junior Fellowship. GC is grateful for the contribution of a grant from the Fédération des Maladies Orphelines (Paris). We would also like to thank Assoc. Prof. M. Simurdová for helpful comments on the manuscript.

Table and figure legends

Table 1. Fractions of membrane currents within the TATS. $C_{m,t}$: specific capacitance of tubular membrane; $fS_{m,t}$: fraction of cell membrane within TATS; $fI_{x,t}$: fraction of individual ion currents in TATS. Column 1: fractions obtained from loss of membrane capacitance and membrane currents after detubulation of rat ventricular myocytes. Column 2: values used in original rat model (see Pasek et al., 2006, and figure 1 legend for further information). Column 3: fractions used in the modified rat model: specific capacitance of the TATS membrane and the fraction of the cell membrane within the TATS were reduced to reconcile estimates of the fraction of cell membrane within the TATS obtained from optical measurements (65 - 49% Soeller and Cannell, 1999) with those obtained using detubulation (32% Despa et al. 2003). See Pasek et al. (2007a) for further details; the analysis of Pasek et al. suggests that these are currently the best estimates of the true values of these variables. The fractions of membrane currents in the TATS of the modified model were those able to reproduce experimental data obtained using detubulation. They differ from the fractions obtained experimentally because of small but unavoidable factors present in experimental conditions that result in the measured fraction differing from the true fraction. These factors include incomplete detubulation, changes of tubular ion concentrations during current measurement, interference from other incompletely blocked currents and small deviations of membrane voltage due to incompletely compensated series resistance (see Pasek et al., 2007a for further detail). Thus the (“true”) fractions in the modified model reproduce the values measured experimentally after these effects are taken into account. The percentage of each current in the surface membrane = 100 minus that shown in the table. Both settings of the model provide a total capacitance:cell volume ratio in the range published by Satoh et al. (1996).

Figure 1. Schematic diagram of a ventricular cell model including TATS. The black dashed arrow denotes ion diffusion between the bulk extracellular space and TATS lumen and the red arrows indicate intracellular Ca pathways. NSR and JSR stand for network and junctional compartments of sarcoplasmic reticulum, B denotes Ca buffers. Individual currents are not shown because these are different in the rat and guinea-pig models referred to in the text; for full descriptions of the models see Pasek et al. (2006, rat; 2007b, guinea-pig). Each current was distributed between the surface and TATS membranes using functional data obtained using detubulation, when available: see table 1 for distribution in rat. Note, however, that other currents are present in the model but not included in the table, which includes only those currents discussed in this review. When detubulation data were not available, immunolabeling or immunogold data were considered. When no information about distribution was available, channel density was assumed to be the same in the TATS and surface membranes. For further information about the currents included in the model, their distribution and formulation, see Pasek et al. (2006; 2007b).

Figure 2. Simulation of the effect of detubulation on the action potential in a rat cardiac myocyte. **A:** Experimental results from Brette et al. (2006c). **B:** Computed results using the model (Pasek et al., 2006). In contrast to the experiment, the model allows computation of the time course of the action potential of each membrane when they were electrically uncoupled (circulation current I_{circ} forced to zero). The uncoupled surface membrane reproduces the short AP after detubulation; the intermediate duration of the compound AP is due to averaging with the longer duration AP of the uncoupled tubular membrane, due to tight electrical coupling.

Figure 3. Steady state (5 Hz) simulation of action potentials (V_m), Ca concentration in network compartment of sarcoplasmic reticulum ($[Ca]_{\text{NSR}}$), cytoplasm ($[Ca]_i$) and lumen of TATS ($[Ca]_t$) obtained using the different rat model settings given in table 1. Full lines represent results from the original model (Pasek et al., 2006); dashed lines: specific membrane capacitance and fractional area of TATS altered; dotted lines: fractions of individual ion currents in TATS also altered. Dashed-dotted straight line in the bottom panel shows external $[Ca]$.

Figure 4. Changes of $[Ca]$ in the peripheral (solid lines), central (dashed lines) and deep (dotted lines) sections of a 10 μm long tubule following a step increase of Ca in the bulk extracellular solution from 0 to 1 mM. The black lines are the same in each panel and show the response using a uniform diameter of 300 nm and a “slow” diffusion coefficient of $0.95 \cdot 10^{-6} \text{ cm}^2/\text{s}$ (see text for further details). The red lines show the effect of increasing the diffusion coefficient to $7.9 \cdot 10^{-6} \text{ cm}^2/\text{s}$ (see text) with uniform or variable diameter along the tubule, as shown by the pictures on the right. The diameter of the peripheral section was reduced to 100 nm (second and fourth panels) and that of the deep part increased to 450 nm (third and fourth panels).

Figure 5. Localization of Kir6.2 ($I_{K_{\text{ATP}}}$), Kir2.1 (I_{K1}) and α -actinin in a rat cardiac myocyte. A1, B1: α -actinin (red) is present only at the Z lines; Kir6.2 is shown in green in A1, Kir2.1 is shown in green in B1. Co-localization of either channel with α -actinin was analysed using fluorograms (A2 and B2) as described by Demandolx and Davoust (1997). The intensity of each pixel of the fluorescence image of K^+ channel labeling (green, ordinate) is plotted against the intensity of the same pixel of the fluorescence image of α -actinin labeling (red, abscissa). Each axis is a linear scale from 0 to 255. For each pixel of the fluorogram, the green and red intensities of original pixels were kept. As the blue layer of the fluorogram image was empty, it was used to indicate the local surface density of pixels in the fluorogram, encoded along a logarithmic scale from 0 to 255 (the more intense the blue color, the higher the local density). Pixels within the white rectangles in A2 and B2 were used to evaluate the colocalization of the two markers as the ratio of the number of pixels bearing both red and green fluorescence to the total number of pixels. There was 47% colocalisation for Kir6.2 and α -actinin (A2) and 49% for Kir2.1 and α -actinin (B2). Horizontal bar (20 μm) in A1 also applies to B1.

Figure 6. Effect of ion concentrations in the TATS on guinea-pig action potentials elicited from resting state in control conditions and following activation of $I_{K_{\text{ATP}}}$ by a decrease of intracellular $[ATP]$ from 6.8 to 1 and 0.5

mM. Solid lines represent action potentials from the model with ion concentrations allowed to vary in the TATS; dashed lines show action potentials from the model when ion concentrations in the TATS were fixed at extracellular levels ($[Ca]_e = 1.8$ mM, $[K^+]_e = 5.4$ mM, $[Na^+]_e = 140$ mM). The conductivity of ATP-dependent K channels at 0 mM intracellular [ATP] and 4 mM external [K] was set to 3.9 mS/cm² (Shaw and Rudy, 1997).

References

- Amsellem, J., Delorme, R., Souchier, C., Christé, G., Bernengo, J.C., Ojeda, C., 1994. 3D reconstruction of transverse tubular membrane system in guinea-pig cardiac ventricular cells: its possible implication in K^+ accumulation-depletion phenomena. *ICEM 13*, 183-184.
- Amsellem, J., Delorme, R., Souchier, C., Ojeda, C., 1995. Transverse-axial tubular system in guinea pig ventricular cardiomyocyte: 3D reconstruction, quantification and its possible role in K^+ accumulation-depletion phenomenon in single cells. *Biol. Cell* 85, 43-54.
- Attwell, D., Cohen, I., Eisner, D., 1979. Membrane potential and ion concentration stability conditions for a cell with restricted extracellular space. *Proc. R. Soc. Lond.* 206, 145-161.
- Balijepalli, R.C., Lokuta, A.J., Maertz, N.A., Buck, J.M., Haworth, R.A., Valdivia, H.H., Kamp, T.J., 2003. Depletion of T-tubules and specific subcellular changes in sarcolemmal proteins in tachycardia-induced heart failure. *Cardiovasc. Res.* 59, 67-77.
- Bassingthwaighte, J.B., 2000. Strategies for the physiome project. *Ann. Biomed. Eng.* 28, 1043-1058.
- Bassingthwaighte, J.B. and Vinnakota, K.C., 2004. The computational integrated myocyte: a view into the virtual heart. *Ann. N. Y. Acad. Sci.* 1015:391-404., 391-404.
- Beard, D.A., 2001. Computational framework for generating transport models from databases of microvascular anatomy. *Ann. Biomed. Eng.* 29, 837-843.
- Beard, D.A., Bassingthwaighte, J.B., Greene, A.S., 2005. Computational modeling of physiological systems. *Physiol. Genomics* 23, 1-3.
- Bers, D.M., 1983. Early transient depletion of extracellular Ca during individual cardiac muscle contractions. *Am. J. Physiol.* 244, H462-H468.
- Blatter, L.A. and Niggli, E., 1998. Confocal near-membrane detection of calcium in cardiac myocytes. *Cell Calcium* 23, 269-279.
- Brette, F. and Orchard, C., 2003. T-tubule function in mammalian cardiac myocytes. *Circ. Res.* 92, 1182-1192.
- Brette, F. and Orchard, C.H., 2006a. Density and sub-cellular distribution of cardiac and neuronal sodium channel isoforms in rat ventricular myocytes. *Biochem. Biophys. Res. Commun.* 348, 1163-1166.
- Brette, F. and Orchard, C.H., 2006b. No apparent requirement for neuronal sodium channels in excitation-contraction coupling in rat ventricular myocytes. *Circ. Res.* 98, 667-674.
- Brette, F., Rodriguez, P., Komukai, K., Colyer, J., Orchard, C.H., 2004a. beta-adrenergic stimulation restores the Ca transient of ventricular myocytes lacking t-tubules. *J. Mol. Cell Cardiol.* 36, 265-275.

- Brette, F., Sallé, L., Orchard, C.H., 2004b. Differential modulation of L-type Ca²⁺ current by SR Ca²⁺ release at the T-tubules and surface membrane of rat ventricular myocytes. *Circ. Res.* 95, e1-e7.
- Brette, F., Sallé, L., Orchard, C.H., 2006c. Quantification of calcium entry at the T-tubules and surface membrane in rat ventricular myocytes. *Biophys. J.* 90, 381-389.
- Caillé, J., Ildefonse, M., Rougier, O., 1985. Excitation-contraction coupling in skeletal muscle. *Prog. Biophys. Mol. Biol.* 46, 185-239.
- Calaghan, S. and White, E., 2006. Caveolae modulate excitation-contraction coupling and beta₂-adrenergic signalling in adult rat ventricular myocytes. *Cardiovasc. Res.* 69, 816-824.
- Cannell, M.B., Crossman, D.J., Soeller, C., 2006. Effect of changes in action potential spike configuration, junctional sarcoplasmic reticulum micro-architecture and altered t-tubule structure in human heart failure. *J. Muscle Res. Cell Motil.* 27, 297-306.
- Christé, G., 1999. Localization of K⁺ channels in the T-tubules of cardiomyocytes as suggested by the parallel decay of membrane capacitance, I_{K1} and I_{KATP} during culture and by delayed I_{K1} response to barium. *J. Mol. Cell. Cardiol.* 31, 2207-2213.
- Christé, G., Simurda, J., Orchard, C., Pasek, M., 2005. Cycling of cations between T-tubular and surface membranes in a model of guinea-pig ventricular cardiomyocyte. *J. Mol. Cell. Cardiol.* 39, 174.
- Clark, R.B., Tremblay, A., Melnyk, P., Allen, B.G., Giles, W.R., Fiset, C., 2001. T-tubule localization of the inward rectifier K⁺ channel in mouse ventricular myocytes: a role in K⁺ accumulation. *J. Physiol. (Lond.)* 537.3, 979-992.
- Cole, W.C., McPherson, C.D., Sontag, D., 1991. ATP-regulated K⁺ channels protect the myocardium against ischemia/reperfusion damage. *Circ. Res.* 69, 571-581.
- Crampin, E.J., Halstead, M., Hunter, P., Nielsen, P., Noble, D., Smith, N., Tawhai, M., 2004. Computational physiology and the Physiome Project. *Exp. Physiol.* 89, 1-26.
- Daut, J., 1982. The passive electrical properties of guinea-pig ventricular muscle as examined with a voltage-clamp technique. *J. Physiol. (Lond.)* 330, 221-242.
- Davare, M.A., Avdonin, V., Hall, D.D., Peden, E.M., Burette, A., Weinberg, R.J., Horne, M.C., Hoshi, T., Hell, J.W., 2001. A beta₂ adrenergic receptor signaling complex assembled with the Ca²⁺ channel Cav1.2. *Science* 293, 98-101.
- Demandolx, D. and Davoust, J., 1997. Multicolour analysis and local image correlation in confocal microscopy. *J. Microscopy* 185, 21-36.
- Dos Remedios, C.G., Liew, C.C., Allen, P.D., Winslow, R.L., Van Eyk, J.E., Dunn, M.J., 2003. Genomics, proteomics and bioinformatics of human heart failure. *J. Muscle Res. Cell Motil.* 24, 251-260.
- Ferrero, J.M., Saiz, J., Thakor, N.V., 1996. Simulation of action potentials from metabolically impaired cardiac myocytes. Role of ATP-sensitive K⁺ current. *Circ. Res.* 79, 208-221.

- Fowler, M.R., Orchard, C.H., Harrison, S.M., 2006. Cellular distribution of calcium current is unaltered during compensated hypertrophy in the spontaneously hypertensive rat. *Pflugers Arch.*, In press.
- Franzini-Armstrong, C., Protasi, F., Ramesh, V., 1999. Shape, size, and distribution of Ca²⁺ release units and couplons in skeletal and cardiac muscles. *Biophys. J.* 77, 1528-1539.
- Freygang, W.H., Goldstein, D.A., Hellam, D.C., 1964. The after-potential that follows trains of impulses in frog muscle fibers. *J. Gen. Physiol.* 47, 929-952.
- Friedrich, O., Ehmer, T., Uttenweiler, D., Vogel, M., Barry, P.H., Fink, R.H.A., 2001. Numerical analysis of Ca²⁺ depletion in the transverse tubular system of mammalian muscle. *Biophys. J.* 80, 2046-2055.
- Gao, Z., Xu, H., Disilvestre, D., Halperin, V.L., Tunin, R., Tian, Y., Yu, W., Winslow, R.L., Tomaselli, G.F., 2005. Transcriptomic profiling of the canine tachycardia-induced heart failure model: global comparison to human and murine heart failure. *J. Mol. Cell. Cardiol.* 40, 76-86.
- Goel, M., Zuo, C.D., Sinkins, W.G., Schilling, W.P., 2006. TRPC3 channels co-localize with the Na⁺, Ca²⁺ exchanger and the Na⁺ pump in the axial component of the transverse-axial-tubular system (TATS) of rat ventricle. *Am. J. Physiol Heart Circ. Physiol.* In press.
- Gomez, A.M., Guatimosim, S., Dilly, K.W., Vassort, G., Lederer, W.J., 2001. Heart failure after myocardial infarction: altered excitation-contraction coupling. *Circulation* 104, 688-693.
- Grantham, C.J. and Cannell, M.B., 1996. Ca²⁺ influx during the cardiac action potential in guinea pig ventricular myocytes. *Circ. Res.* 79, 194-200.
- He, J.Q., Conklin, M., Foell, J.D., Wolff, M.R., Haworth, R.A., Coronado, R., Kamp, T.J., 2001. Reduction in density of transverse tubules and L-type Ca²⁺ channels in canine tachycardia-induced heart failure. *Cardiovasc. Res.* 49, 298-307.
- Hunter, P. and Nielsen, P., 2005. A strategy for integrative computational physiology. *Physiology (Bethesda)*. 20, 316-325.
- Hunter, P., Robbins, P., Noble, D., 2002. The IUPS human physiome project. *Pflugers Arch.* 445, 1-9.
- Knopp, A., Thierfelder, S., Koopmann, R., Biskup, C., Bohle, T., Benndorf, K., 1999. Anoxia generates rapid and massive opening of KATP channels in ventricular cardiac myocytes. *Cardiovasc. Res.* 41, 629-640.
- Korchev, Y.E., Negulyaev, Y.A., Edwards, C.R.W., Vodyanov, I., Lab, M.J., 2000. Functional localization of single active ion channels on the surface of a living cell. *Nature Cell Biol.* 2, 616-619.
- Kostin, S., Scholz, D., Shimada, T., Maeno, Y., Mollnau, H., Hein, S., Schaper, J., 1998. The internal and external protein scaffold of the T-tubular system in cardiomyocytes. *Cell Tissue Res.* 294, 449-460.
- Laflamme, M.A. and Becker, P.L., 1999. G(s) and adenylyl cyclase in transverse tubules of heart: implications for cAMP-dependent signaling. *Am. J. Physiol.* 277, H1841-H1848.

- Louch, W.E., Bito, V., Heinzl, F.R., Macianskiene, R., Vanhaecke, J., Flameng, W., Mubagwa, K., Sipido, K., Sipido, K.R., 2004. Reduced synchrony of Ca²⁺ release with loss of T-tubules - a comparison to Ca²⁺ release in human failing cardiomyocytes. *Cardiovasc. Res.* 62, 63-73.
- Marcus, 1997. Ion transport. In: Dekker Marcel (Ed.), *Ion properties*. Marcel Dekker, New York, pp. 159-176.
- Marks, A.R., 2003. A guide for the perplexed: towards an understanding of the molecular basis of heart failure. *Circulation* 107, 1456-1459.
- Nichols, C.G. and Lederer, W.J., 1991. ATP-sensitive potassium channel modulation of the guinea pig ventricular action potential and contraction. *Circ. Res.* 68, 280-287.
- Page, E., 1978. Quantitative ultrastructural analysis in cardiac membrane physiology. *Am. J. Physiol.* 235, C147-C158.
- Pasek, M., Brette, F., Nelson, D.A., Pearce, C., Qaiser, A., Christé, G., Orchard, C., 2007a. Quantification of t-tubule area and protein distribution in rat cardiac ventricular myocytes. *Prog. Biophys. Mol. Biol.* Present issue.
- Pasek, M., Christé, G., Simurda, J., 2002. Arrhythmogenic effect of extracellular K⁺-depletion is prevented by the transverse-axial tubular system in a ventricular cardiac cell model. *Scripta Medica* 75, 179-186.
- Pasek, M., Christé, G., Simurda, J., 2003. A quantitative model of cardiac ventricular cell incorporating the transverse-axial tubular system. *Gen. Physiol. Biophys.* 22, 355-368.
- Pasek, M., Simurda, J., Christé, G., 2006. The functional role of cardiac T-tubules explored in a model of rat ventricular myocytes. *Philos. Transact. A Math. Phys. Eng. Sci.* 364, 1187-1206.
- Pasek, M., Simurda, J., Orchard, C.H., Christé, G., 2007b. A model of the guinea-pig ventricular cardiomyocyte incorporating a transverse-axial tubular system. *Prog. Biophys. Mol. Biol.* Present issue.
- Pouvreau, S., Berthier, C., Blaineau, S., Amsellem, J., Coronado, R., Strube, C., 2004. Membrane cholesterol modulates dihydropyridine receptor function in mice fetal skeletal muscle cells. *J. Physiol. (Lond)* 555, 365-381.
- Puglisi, J.L., Wang, F., Bers, D.M., 2004. Modeling the isolated cardiac myocyte. *Prog. Biophys. Mol. Biol.* 85, 163-178.
- Quinn, F.R., Currie, S., Duncan, A.M., Miller, S., Sayeed, R., Cobbe, S.M., Smith, G.L., 2003. Myocardial infarction causes increased expression but decreased activity of the myocardial Na⁺-Ca²⁺ exchanger in the rabbit. *J. Physiol.* 553, 229-242.
- Roseblatt, M., Hidalgo, C., Vergara, C., Ikemoto, N., 1981. Immunological and biochemical properties of transverse tubule membranes isolated from rabbit skeletal muscle. *J. Biol. Chem.* 256, 8140-8148.

- Satoh, H., Delbridge, L.M.D., Blatter, L.A., Bers, D.M., 1996. Surface:volume relationship in cardiac myocytes studied with confocal microscopy and membrane capacitance measurements: species-dependence and developmental effects. *Biophys. J.* 70, 1494-1504.
- Schroder, F., Handrock, R., Beuckelmann, D.J., Hirt, S., Hullin, R., Priebe, L., Schwinger, R.H., Weil, J., Herzig, S., 1998. Increased availability and open probability of single L-type calcium channels from failing compared with nonfailing human ventricle. *Circulation* 98, 969-976.
- Scriven, D.R., Klimek, A., Lee, K.L., Moore, E.D., 2002. The molecular architecture of calcium microdomains in rat cardiomyocytes. *Ann. N. Y. Acad. Sci.* 976, 488-499.
- Shaw, R. and Rudy, Y., 1997. Electrophysiologic effects of acute myocardial ischemia: a mechanistic investigation of action potential conduction and conduction failure. *Circ. Res.* 80, 124-138.
- Shepherd, N. and McDonough, H.B., 1998. Ionic diffusion in transverse tubules of cardiac ventricular myocytes. *Am. J. Physiol.* 275, H852-H860.
- Simons, K. and Eehalt, R., 2002. Cholesterol, lipid rafts, and disease. *J. Clin. Invest.* 110, 597-603.
- Simurda, J., Pasek, M., Christé, G., Simurdova, M., 2004. Modelling the distribution of $[Ca^{2+}]$ within the cardiac T-tubule - Effects of Ca^{2+} current distribution and changes in extracellular $[Ca^{2+}]$. *J. Physiol. (Lond)* 561P, 13P.
- Sipido, K.R. and Eisner, D., 2005. Something old, something new: changing views on the cellular mechanisms of heart failure. *Cardiovasc. Res.* 68, 167-174.
- Soeller, C. and Cannell, M.B., 1999. Examination of the transverse tubular system in living cardiac rat myocytes by 2-photon microscopy and digital image-processing techniques. *Circ. Res.* 84, 266-275.
- Song, L.S., Guatimosim, S., Gomez-Viquez, L., Sobie, E.A., Ziman, A., Hartmann, H., Lederer, W.J., 2005. Calcium biology of the transverse tubules in heart. *Ann. N. Y. Acad. Sci.* 1047, 99-111.
- Song, L.S., Sobie, E.A., McCulle, S., Lederer, W.J., Balke, C.W., Cheng, H., 2006. Orphaned ryanodine receptors in the failing heart. *Proc. Natl. Acad. Sci. U. S. A.* 103, 4305-4310.
- Sumnicht, G.E. and Sabbadini, R.A., 1982. Lipid composition of transverse tubular membranes from normal and dystrophic skeletal muscle. *Arch. Biochem. Biophys.* 215, 628-637.
- Swift, F., Stromme, T.A., Amundsen, B., Sejersted, O.M., Sjaastad, I., 2006. Slow diffusion of K^+ in the T tubules of rat cardiomyocytes. *J. Appl. Physiol.* 101, 1170-1176.
- Thomas, M.J., Sjaastad, I., Andersen, K., Helm, P.J., Wasserstrom, J.A., Sejersted, O.M., Ottersen, O.P., 2003. Localization and function of the Na^+/Ca^{2+} exchanger in normal and detubulated rat cardiomyocytes. *J. Mol. Cell. Cardiol.* 35, 1325-1337.
- Tourneur, Y., Marion, A., Gautier, P., 1994. SR47063, a potent channel opener, activates K_{ATP} and a time- dependent current likely due to potassium accumulation. *J. Membr. Biol.* 142, 337-347.
- Wallinga, W., Meijer, S.L., Alberink, M.J., Vliek, M., Wienk, E.D., Ypey, D.L., 1999. Modelling action potentials and membrane currents of mammalian skeletal muscle fibres in coherence with potassium concentration changes in the T-tubular system. *Eur. Biophys. J.* 28, 317-329.

- Wehrens, X.H. and Marks, A.R., 2004. Molecular determinants of altered contractility in heart failure. *Ann. Med.* 36 Suppl 1, 70-80.
- Weiss, J.N. and Venkatesh, N., 1993. Metabolic regulation of cardiac ATP-sensitive K⁺ channels. *Cardiovasc. Drugs Ther.* 7, 499-505.
- Winslow, R.L., Scollan, D.F., Holmes, A., Yung, C.K., Zhang, J., Jafri, M.S., 2000. Electrophysiological modeling of cardiac ventricular function: from cell to organ. *Annu. Rev. Biomed. Eng.* 2, 119-55.
- Yao, A., Spitzer, K.W., Ito, N., Zaniboni, M., Lorell, B.H., Barry, W.H., 1997. The restriction of diffusion of cations at the external surface of cardiac myocytes varies between species. *Cell Calcium* 22, 431-438.
- Yasui, K., Anno, T., Kamiya, K., Boyett, M.R., Kodama, I., Toyama, J., 1993. Contribution of potassium accumulation in narrow extracellular spaces to the genesis of nicorandil-induced large inward tail current in guinea-pig ventricular cells. *Pflugers Arch.* 422, 371-379.

| | experimental data | settings in original model | settings in modified model |
|---------------|------------------------------|---------------------------------------|---------------------------------------|
| $C_{m,t}$ | - | $1 \mu\text{F}/\text{cm}^2$ | $0.56 \mu\text{F}/\text{cm}^2$ |
| $fS_{m,t}$ | 32 % | 56 % | 49 % |
| $fI_{Na,t}$ | 32 % | 56 % | 38 % |
| $fI_{Ca,t}$ | 87 % | 87 % | 95 % |
| $fI_{Kto,t}$ | 32 % | 56 % | 46 % |
| $fI_{Kss,t}$ | 76 % | 76 % | 86 % |
| $fI_{Kl,t}$ | 32 % | 56 % | 47 % |
| $fI_{NaCa,t}$ | 63 % | 81 % | 78 % |
| $fI_{NaK,t}$ | 59 % | 59 % | 64 % |
| $fI_{pCa,t}$ | - | 56 % | 49 % |

Table 1. Fractions of membrane currents within the TATS. $C_{m,t}$: specific capacitance of tubular membrane; $fS_{m,t}$: fraction of cell membrane within TATS; $fI_{x,t}$: fraction of individual ion currents in TATS. Column 1: fractions obtained from loss of membrane capacitance and membrane currents after detubulation of rat ventricular myocytes. Column 2: values used in original rat model (see Pasek et al., 2006, and figure 1 legend for further information). Column 3: fractions used in the modified rat model: specific capacitance of the TATS membrane and the fraction of the cell membrane within the TATS were reduced to reconcile estimates of the fraction of cell membrane within the TATS obtained from optical measurements (65 - 49% Soeller and Cannell, 1999) with those obtained using detubulation (32% Despa et al. 2003). See Pasek et al. (2007a) for further details; the analysis of Pasek et al. suggests that these are currently the best estimates of the true values of these variables. The fractions of membrane currents in the TATS of the modified model were those able to reproduce experimental data obtained using detubulation. They differ from the fractions obtained experimentally because of small but unavoidable factors present in experimental conditions that result in the measured fraction differing from the true fraction. These factors include incomplete detubulation, changes of tubular ion concentrations during current measurement, interference from other incompletely blocked currents and small deviations of membrane voltage due to incompletely compensated series resistance (see Pasek et al., 2007a for further detail). Thus the (“true”) fractions in the modified model reproduce the values measured experimentally after these effects are taken into account. The percentage of each current in the surface membrane = 100 minus that shown in the table. Both settings of the model provide a total capacitance:cell volume ratio in the range published by Satoh et al. (1996).

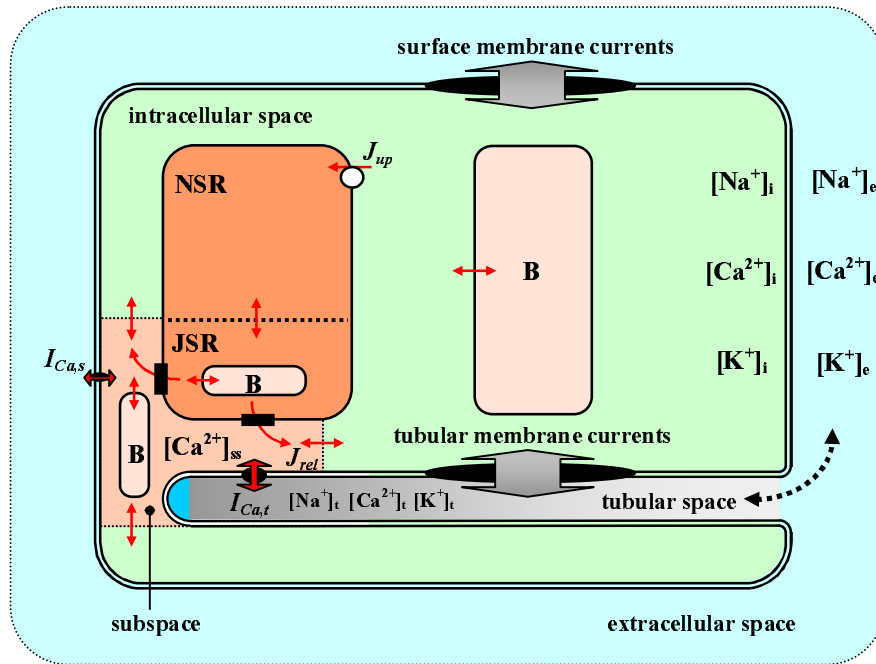


Figure 1. Schematic diagram of a ventricular cell model including TATS. The black dashed arrow denotes ion diffusion between the bulk extracellular space and TATS lumen and the red arrows indicate intracellular Ca pathways. NSR and JSR stand for network and junctional compartments of sarcoplasmic reticulum, B denotes Ca buffers. Individual currents are not shown because these are different in the rat and guinea-pig models referred to in the text; for full descriptions of the models see Pasek et al. (2006, rat; 2007b, guinea-pig). Each current was distributed between the surface and TATS membranes using functional data obtained using detubulation, when available: see table 1 for distribution in rat. Note, however, that other currents are present in the model but not included in the table, which includes only those currents discussed in this review. When detubulation data were not available, immunolabeling or immunogold data were considered. When no information about distribution was available, channel density was assumed to be the same in the TATS and surface membranes. For further information about the currents included in the model, their distribution and formulation, see Pasek et al. (2006; 2007b).

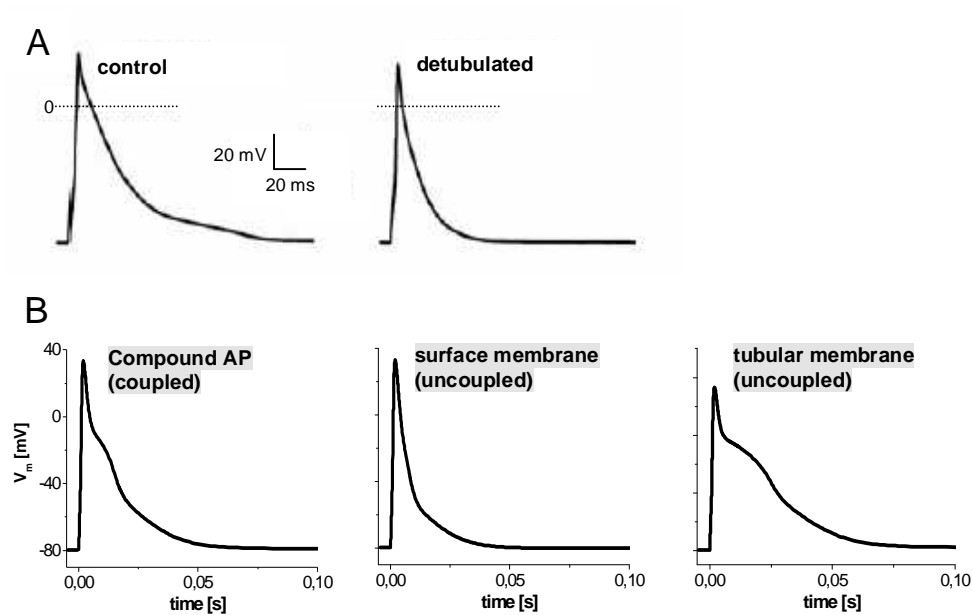


Figure 2. Simulation of the effect of detubulation on the action potential in a rat cardiac myocyte. **A:** Experimental results from Brette et al. (2006c). **B:** Computed results using the model (Pasek et al., 2006). In contrast to the experiment, the model allows computation of the time course of the action potential of each membrane when they were electrically uncoupled (circulation current I_{circ} forced to zero). The uncoupled surface membrane reproduces the short AP after detubulation; the intermediate duration of the compound AP is due to averaging with the longer duration AP of the uncoupled tubular membrane, due to tight electrical coupling.

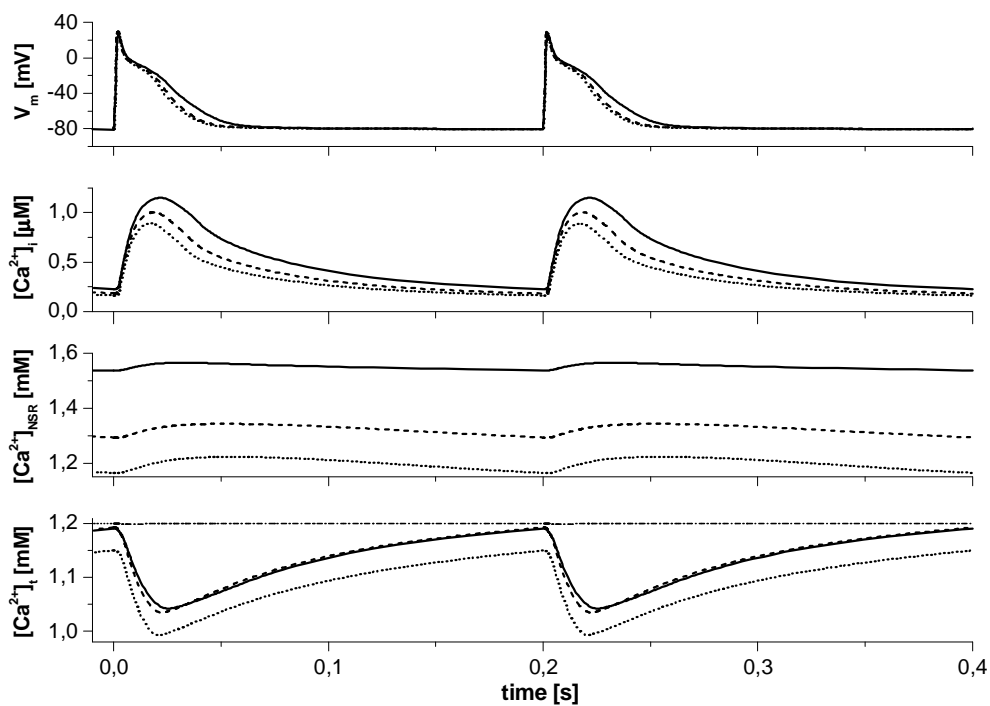


Figure 3. Steady state (5 Hz) simulation of action potentials (V_m), Ca concentration in network compartment of sarcoplasmic reticulum ($[Ca]_{NSR}$), cytoplasm ($[Ca]_i$) and lumen of TATS ($[Ca]_l$) obtained using the different rat model settings given in table 1. Full lines represent results from the original model (Pasek et al., 2006); dashed lines: specific membrane capacitance and fractional area of TATS altered; dotted lines: fractions of individual ion currents in TATS also altered. Dashed-dotted straight line in the bottom panel shows external $[Ca]$.

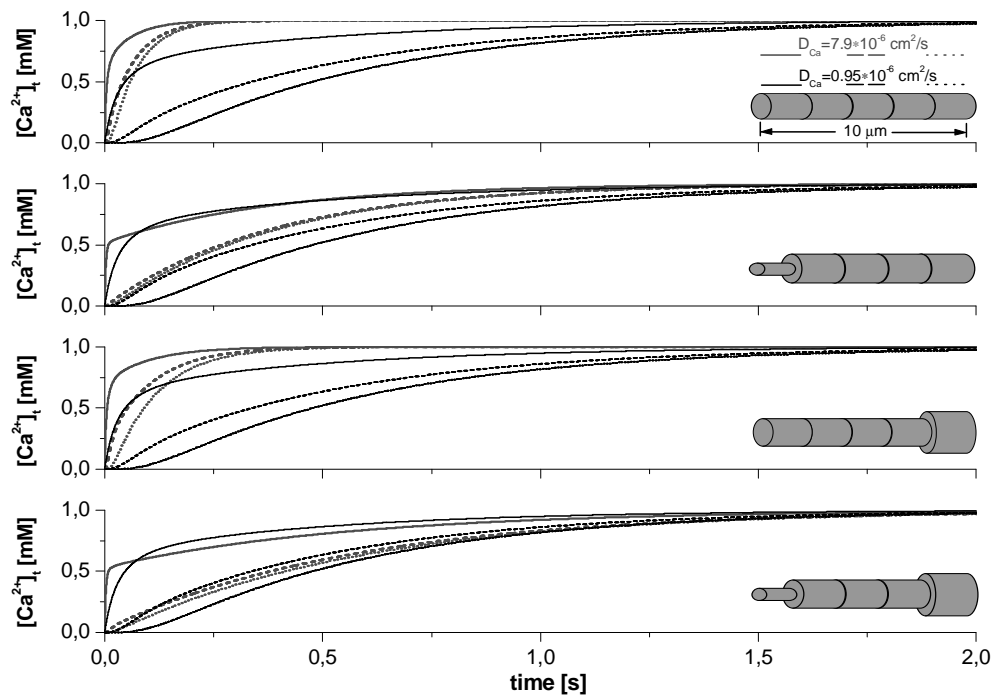


Figure 4. Changes of $[Ca]_i$ in the peripheral (solid lines), central (dashed lines) and deep (dotted lines) sections of a $10\ \mu\text{m}$ long tubule following a step increase of Ca in the bulk extracellular solution from 0 to $1\ \text{mM}$. The black lines are the same in each panel and show the response using a uniform diameter of $300\ \text{nm}$ and a “slow” diffusion coefficient of $0.95 \cdot 10^{-6}\ \text{cm}^2/\text{s}$ (see text for further details). The red lines show the effect of increasing the diffusion coefficient to $7.9 \cdot 10^{-6}\ \text{cm}^2/\text{s}$ (see text) with uniform or variable diameter along the tubule, as shown by the pictures on the right. The diameter of the peripheral section was reduced to $100\ \text{nm}$ (second and fourth panels) and that of the deep part increased to $450\ \text{nm}$ (third and fourth panels).

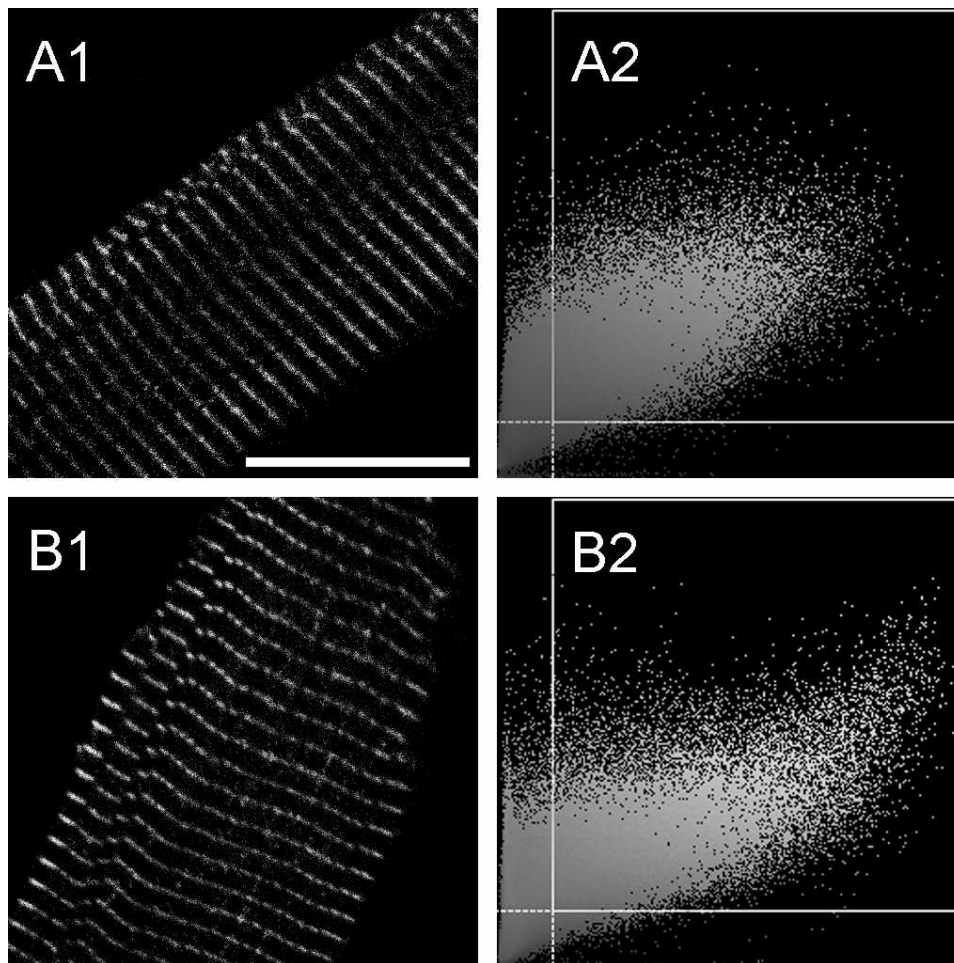


Figure 5. Localization of Kir6.2 ($I_{K,ATP}$), Kir2.1 (I_{K1}) and α -actinin in a rat cardiac myocyte. A1, B1: α -actinin (red) is present only at the Z lines; Kir6.2 is shown in green in A1, Kir2.1 is shown in green in B1. Colocalization of either channel with α -actinin was analysed using fluorograms (A2 and B2) as described by Demandolx and Davoust (1997). The intensity of each pixel of the fluorescence image of K^+ channel labeling (green, ordinate) is plotted against the intensity of the same pixel of the fluorescence image of α -actinin labeling (red, abscissa). Each axis is a linear scale from 0 to 255. For each pixel of the fluorogram, the green and red intensities of original pixels were kept. As the blue layer of the fluorogram image was empty, it was used to indicate the local surface density of pixels in the fluorogram, encoded along a logarithmic scale from 0 to 255 (the more intense the blue color, the higher the local density). Pixels within the white rectangles in A2 and B2 were used to evaluate the colocalization of the two markers as the ratio of the number of pixels bearing both red and green fluorescence to the total number of pixels. There was 47% colocalisation for Kir6.2 and α -actinin (A2) and 49% for Kir2.1 and α -actinin (B2). Horizontal bar (20 μ m) in A1 also applies to B1.

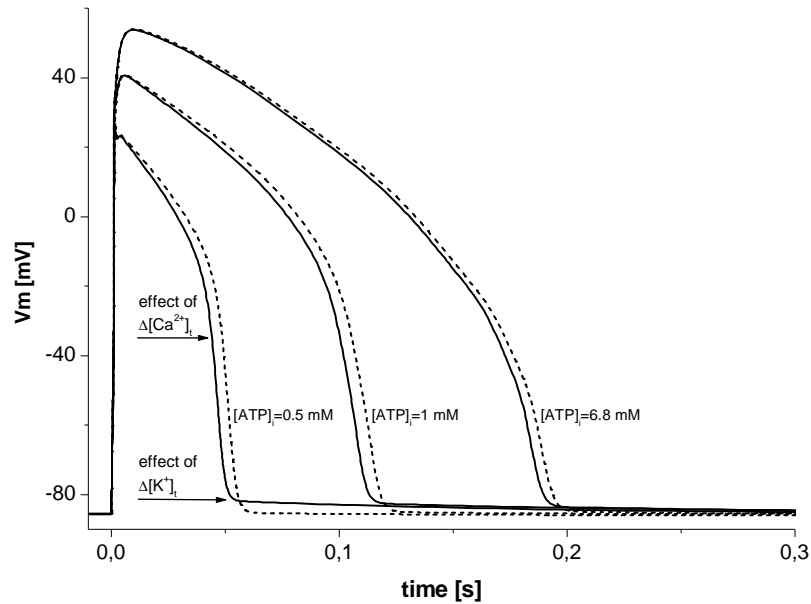


Figure 6. Effect of ion concentrations in the TATS on guinea-pig action potentials elicited from resting state in control conditions and following activation of $I_{K,ATP}$ by a decrease of intracellular [ATP] from 6.8 to 1 and 0.5 mM. Solid lines represent action potentials from the model with ion concentrations allowed to vary in the TATS; dashed lines show action potentials from the model when ion concentrations in the TATS were fixed at extracellular levels ($[Ca]_e = 1.8$ mM, $[K^+]_e = 5.4$ mM, $[Na^+]_e = 140$ mM). The conductivity of ATP-dependent K channels at 0 mM intracellular [ATP] and 4 mM external [K] was set to 3.9 mS/cm² (Shaw & Rudy, 1997).